



Citation for published version:

Courtney, CRP, Neild, SA, Wilcox, PD & Drinkwater, BW 2010, 'Application of the bispectrum for detection of small nonlinearities excited sinusoidally', *Journal of Sound and Vibration*, vol. 329, no. 20, pp. 4279-4293.
<https://doi.org/10.1016/j.jsv.2010.04.031>

DOI:

[10.1016/j.jsv.2010.04.031](https://doi.org/10.1016/j.jsv.2010.04.031)

Publication date:

2010

Document Version

Peer reviewed version

[Link to publication](#)

Publisher Rights

Unspecified

NOTICE: this is the author's version of a work that was accepted for publication in *Journal of Sound and Vibration*. Changes resulting from the publishing process, such as peer review, editing, corrections, structural formatting, and other quality control mechanisms may not be reflected in this document. Changes may have been made to this work since it was submitted for publication. A definitive version was subsequently published in *Journal of Sound and Vibration*, vol 329, issue 20, DOI 10.1016/j.jsv.2010.04.031

University of Bath

General rights

Copyright and moral rights for the publications made accessible in the public portal are retained by the authors and/or other copyright owners and it is a condition of accessing publications that users recognise and abide by the legal requirements associated with these rights.

Take down policy

If you believe that this document breaches copyright please contact us providing details, and we will remove access to the work immediately and investigate your claim.

Application of the bispectrum for detection of small non-linearities excited sinusoidally

C. R. P. Courtney, S. A. Neild, P. D. Wilcox, B. W. Drinkwater

Department of Mechanical Engineering, University of Bristol, University Walk, Bristol, BS8 1TR, UK

Abstract

The non-linear behaviour of damaged systems excited by vibration or ultrasound offers potential as a technique for damage detection in machine condition monitoring and non-destructive testing applications. The bispectrum, a third order spectrum, has properties that lend themselves to the measurement of non-linearities in systems. The properties of interest are insensitivity to Gaussian noise and ability to detect quadratic phase coupling. However, thus far analysis of the statistics of bispectrum estimation have been mainly aimed at stochastic systems. Many applications to vibration and ultrasound involve primarily deterministic, periodic excitations in the presence of stochastic noise. This paper considers the properties of a bispectrum estimate when applied to a system with weak quadratic non-linearity excited by the superposition of two sinusoids in the presence of additive Gaussian noise. This is compared, using signal-to-noise ratios, to the powerspectrum, with the results validated using numerical data. Also addressed is the effect of quadratic phase coupling on such a system (in the absence of noise).

Key words: Non-destructive Evaluation, Non-linear, Bispectrum, Intermodulation,

1. Introduction

This paper is concerned with the analysis of periodically excited systems using a third order spectrum, the bispectrum, to identify weak non-linearities for damage detection.

The use of non-linear interactions for damage detection in engineering materials was originally proposed using the measurement of harmonic amplitudes in fatigued aluminium excited with ultrasound [1, 2]. Interest in the measurement of non-linearity as a non-destructive testing tool was re-ignited in 1998 with Nagy's paper [3] on the sensitivity of harmonic generation to microscopic damage. Donskoy et al. [4] later demonstrated an approach using the intermodulation of two frequencies looking at the responses at the sum and difference frequencies. Much work has been published in this area, considering both low frequency vibrations [5–8] and ultrasonic frequencies [9–12]. A review of the research is given in [13].

The commonly used powerspectrum is second order with respect to signal amplitude and results in a frequency-amplitude relationship. The bispectrum is third order and results in a frequency-frequency-amplitude relationship that shows the coupling between signals at different frequencies. Two important properties of the bispectrum [14] have motivated its use in the analysis of non-linear systems: i) the bispectrum of Gaussian noise is zero and ii) the bispectrum detects quadratic phase coupling between frequency components, a signature of quadratic non-linearity.

The use, in 1963, of the bispectrum to analyse the non-linear interaction of ocean waves [15] instigated interest in the bispectrum as a tool for analysing non-linear interactions. Initially interest was in identifying non-linear behaviour in stochastic systems with the technique applied in fields as diverse as oceanography [15], economics [16], electroencephalography [17, 18], fluid mechanics [19] and plasma physics [14]. Consequently the development of the theoretical grounding and computational tools was primarily concerned with the treatment of random processes [17, 20–23].

In 1995 Fackrell et al. [24, 25] considered the properties of bispectra applied to periodic signals with particular attention to using bicoherence (a normalised bispectrum) in machine condition monitoring. Periodic signals were shown to produce a 'bed of nails' form in the bispectrum, with deviations from this form indicative of deviations from periodicity, resulting from damage. This approach was applied to a beam with a loosened nut attaching it to a shaker fed with white noise, a perspex model of a ship's double hull excited by a periodic input and a vacuum cleaner. Howard [26] considered the theory of applying the bicoherence and tricoherence to phase modulated and amplitude modulated periodic signals with a view to using higher order spectra for machine condition monitoring and demonstrated that for inputs of frequency f_c modulated in phase or amplitude at frequency f_m the bicoherence approached unity for coupled frequency pairs ($f_m, f_c - f_m$ for example) and zero for other frequencies. It was noted that, in theory, other signals occurring at these pairs of frequencies, but not phase coupled, would not appear in the bicoherence, although this was not demonstrated with the numerical data. Collis et al. [27] demonstrated numerically, using narrow-band-filtered Gaussian inputs, that the bispectrum could distinguish quadratically-phase-coupled signals generated by a quadratic non-linearity from signals having the same powerspectrum, but uncorrelated phases. The bispectrum (and the bicoherence) was applied by Boltežar et al. [28] to the dynamics of washing machines, demonstrating that certain excited modes of the oscillation could be associated with quadratic phase coupling. It has been demonstrated

experimentally that the bispectrum can be used to monitor the increase in second harmonic generation by a rotating axle which is cracked or misaligned [29].

The application of bispectral analysis to detection of fatigue cracks was suggested by Rivola and White [30]. The concept, that non-linear systems produce harmonics of the driving frequency that result in a non-zero bicoherence, was demonstrated by numerical solutions for a sinusoidally driven bilinear oscillator. Experimentally it was demonstrated that the bicoherence of the acceleration of a bronze beam, excited with white noise by a shaker, was sensitive to cracks introduced into the beam. Hillis et al. developed a test for fatigue cracks in metal engineering parts using the bispectrum peak due to intermodulation of two ultrasonic excitations [11, 31].

Application of the bispectrum to damage detection has involved, in several cases, its use in systems excited sinusoidally. However the theory underpinning the use of the bispectrum has largely been developed for non-periodic stochastic systems, leading to some ambiguity as to the properties of the bispectrum when applied to sinusoidally excited systems and how they may be best exploited. This paper analyses the statistics of bispectrum estimators when a weakly non-linear system is excited at two frequencies in the presence of Gaussian noise. The aim is to quantify any noise suppression effects for these systems and identify how to detect quadratic phase coupling in the system response. For comparison, the statistics of powerspectrum estimators for the same system are also applied. Appropriate signal-to-noise ratios are developed for the comparison of the sensitivity (i.e. the ability to reliably detect small non-linearities) of the bispectrum to that of the powerspectrum.

2. Definitions

For a stationary, random signal $x(t)$ the second-order spectral density (power spectrum) is given by[27]:

$$P(f) = E[X(f)X^*(f)] \quad (1)$$

where $X(f)$ is the Fourier transform of $x(t)$, $E[...]$ indicates the expectation value (or equivalently the average over a statistical ensemble) and $*$ denotes the complex conjugate. The second order spectrum is a widely known and commonly used spectra but it is just one of a family of spectra of increasing order. This paper considers the powerspectrum and the third-order spectrum; the bispectrum. Details of higher order spectra can be found in [32]. The bispectrum is given by

$$B(f_1, f_2) = E[X(f_1)X(f_2)X^*(f_1 + f_2)] \quad (2)$$

These are the direct definitions, each of the spectra can also be written indirectly in terms of autocorrelation functions, see for example [21, 22]. Due to the symmetries in the bispectrum the region bounded by the lines $f_1 = 0$ and $f_1 = f_2$ (shown in Fig. 1) contains all the available information[17, 20, 33]. It is clear from Eq. 2 that if $X(f_1) = 0$, $X(f_2) = 0$ or $X(f_1 + f_2) = 0$ the bispectrum at f_1, f_2 will also be zero. Less obvious is that, for the bispectrum to be non-zero, the phases of these three components must be quadratically phase coupled [21]. This phase relationship is one of the reasons that the bispectrum has excited much interest in the analysis of non-linear systems and will be discussed at a later stage in this paper. In short, signals resulting from the non-linear interaction of some excitation components have a specific phase relationship with the

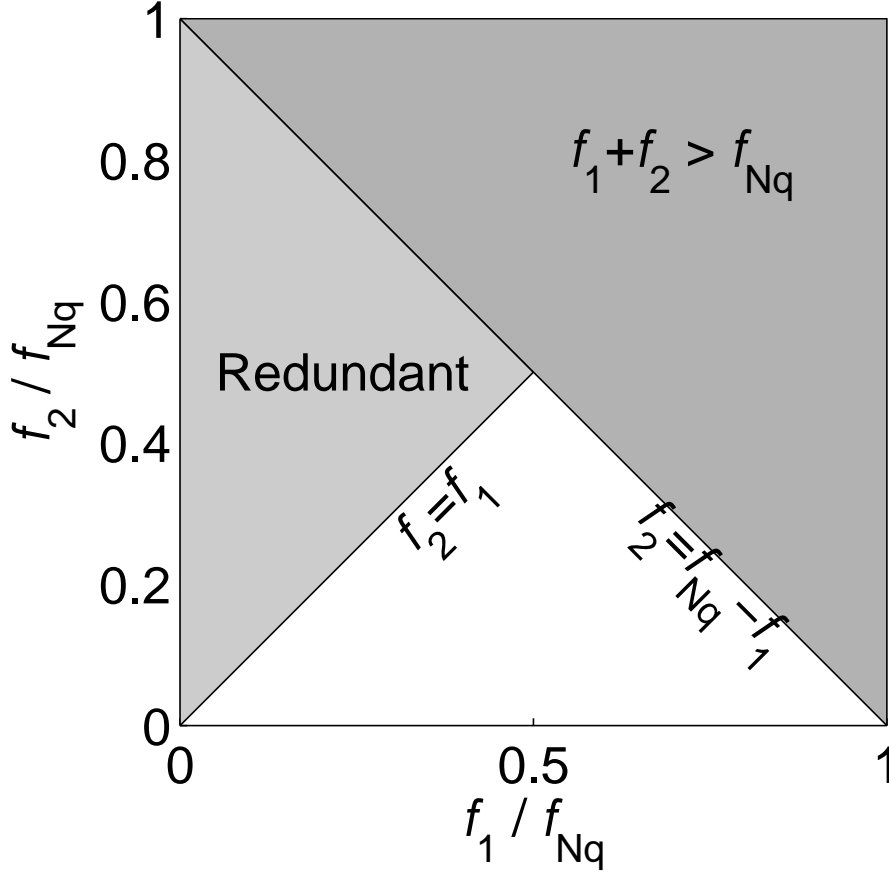


Figure 1: Region of interest for Bispectrum. The frequency field is divided into the region containing useful information (not shaded), a region where the information is redundant due to the symmetry about $f_1 = f_2$ and the part of the region where one of the components (that at $f_1 + f_2$) exceeds the Nyquist frequency, f_{Nq} .

excitations that caused them. In the powerspectrum the phase information is lost and hence this phase relationship between different frequencies cannot be exploited.

Previously the bispectrum has most frequently been defined and discussed in the context of application to random responses, for which there is a great deal of literature from the signal processing community (see for example [17, 20, 21]). However recent applications to machine condition monitoring and non-destructive testing have applied the bispectrum to responses with strong deterministic, periodic components. For a deterministic response (i.e. one which invariably produces a given response, containing no random element) the expectation values in Eqs. 1–2 are redundant (there is only a single possible waveform in the statistical ensemble) and the bispectrum is the product of three Fourier transforms:

$$B(f_1, f_2) = X(f_1)X(f_2)X^*(f_1 + f_2) \quad (3)$$

For purely deterministic responses the quadratic phase coupling feature does not manifest itself.

However, real systems, even where the intention is to use deterministic excitations, produce a mixture of deterministic signals along with stochastic noise. This leads to a second motivation for using the bispectrum; the bispectrum of Gaussian white noise is identically zero and so the bispectrum has potential for the removal of noise from otherwise deterministic sinusoidal signals.

2.1. Estimation

In general the expectation values in Eqs. (1) and (2) need to be estimated from a finite quantity of available data. The most straightforward method of evaluating the spectra is to use a number of different records, calculate an estimate of the required spectrum of each record and then average over those spectra. This approach is taken in this work.

General Procedure. Data consisting of M discrete time series $x_i(t_j)$, each measured at N points ($t_j = j\Delta t$; $j = 1, 2, \dots, N$), is considered. Three spectral estimates are considered: the average power spectrum, the power spectrum of the average response and the bispectrum. The two approaches to estimating the powerspectrum both involve averaging in the frequency domain. The average powerspectrum involves calculating the powerspectrum of each time series, before averaging and the powerspectrum of the average response involves first averaging the frequency domain response over all time series and then calculating the powerspectrum.

The general approach can be summarized in four steps

1. Remove mean of each record, $x_i(t_j)$
2. Perform fast Fourier transform to obtain $X_i(f_k)$, for each record ($x_i(t_j)$) at frequencies $f_k = \frac{1}{n\Delta t}k$ for $k = 1, 2, \dots, N/2$.
3. Calculate appropriate spectrum for each record from $X_i(f_k)$.
4. Average spectrum over M records

The aim, when dealing with stochastic signals is to reduce the variance of the estimate. In this paper averaging over large numbers of records is used to achieve this. Alternative methods include using longer records and averaging in the frequency domain before averaging over the records [17, 22], however the effect on the variance of the bispectrum for a given record length is equivalent to dividing into records [34]. Parametric methods offer an alternative to conventional methods [21], but will not be discussed here.

Estimation of the Powerspectrum. For the powerspectrum, as defined in Eq. (1), the general estimation approach is taken with the powerspectrum for each record calculated and then an average performed:

$$\hat{P}(f_k) = \frac{1}{M} \sum_{i=1}^M X_i(f_k)X_i^*(f_k) \quad (4)$$

For deterministic excitations an alternative method may be applied, in which the time-domain responses are averaged (or equivalently the frequency-domain signals) before the powerspectrum of the average response is calculated:

$$\hat{P}'(f_k) = \frac{1}{M^2} \sum_{i=1}^M X_i(f_k) \sum_{h=1}^M X_h^*(f_k) \quad (5)$$

Estimation of the Bispectrum. The general approach outlined above is taken with the bispectrum calculated for each record and then averaged over all records:

$$\hat{B}(f_l, f_m) = \frac{1}{M} \sum_{i=1}^M X_i(f_l) X_i(f_m) X_i^*(f_l + f_m) \quad (6)$$

Sections 4 and 5 compare the statistics of both these approaches for estimating the powerspectrum with those for bispectrum estimation and demonstrate that the high variance of the bispectrum estimate makes the powerspectrum estimators more reliable for detecting weak non-linearities excited sinusoidally.

2.2. Quadratic non-linear systems

This paper considers quadratically non-linear systems where the response, $x(t)$, for an input $y(t)$ is:

$$x(t) = \alpha y(t) + \beta y^2(t) + q(t), \quad (7)$$

where $q(t)$ is additive Gaussian white noise and α and β are constants that define the linear and non-linear components of the system's input-output relationship.

Applying two sinusoids allows mixing due to non-linearity and harmonic production to be observed. A suitable input is:

$$y(t) = S_1 \sin(2\pi F_1 t + \phi_1) + S_2 \sin(2\pi F_2 t + \phi_2). \quad (8)$$

Substituting Eq. (8) into Eq. (7) and applying trigonometric identities (ignoring terms that are constant in time) gives a response:

$$\begin{aligned} x(t) = & \alpha S_1 \sin(2\pi F_1 t + \phi_1) + \alpha S_2 \sin(2\pi F_2 t + \phi_2) \\ & - \beta \frac{S_1^2}{2} \cos[2\pi(2F_1)t + 2\phi_1] \\ & - \beta \frac{S_2^2}{2} \cos[2\pi(2F_2)t + 2\phi_2] \\ & + \beta S_1 S_2 \cos(2\pi(F_2 - F_1)t + (\phi_2 - \phi_1)) \\ & - \beta S_1 S_2 \cos(2\pi(F_2 + F_1)t + (\phi_2 + \phi_1)) \\ & + q(t) \end{aligned} \quad (9)$$

In the frequency domain (ignoring contributions at negative frequency which fall outside the useful region of the powerspectrum and the bispectrum) this can be written

as:

$$\begin{aligned}
A(f) = \mathcal{F}[x(t)] &= -i\frac{\alpha S_1}{2}\delta(F_1 - f)e^{i\phi_1} - i\frac{\alpha S_2}{2}\delta(F_2 - f)e^{i\phi_2} \\
&\quad - \frac{\beta S_1^2}{4}\delta(2F_1 - f)e^{i2\phi_1} \\
&\quad - \frac{\beta S_2^2}{4}\delta(2F_2 - f)e^{i2\phi_2} \\
&\quad + \frac{\beta S_1 S_2}{2}\delta(F_2 - F_1 - f)e^{i(\phi_2 - \phi_1)} \\
&\quad - \frac{\beta S_1 S_2}{2}\delta(F_2 + F_1 - f)e^{i(\phi_2 + \phi_1)} \\
&\quad + Q(f)
\end{aligned} \tag{10}$$

where $\mathcal{F}[\cdot]$ is the Fourier transform, $Q(f) = \mathcal{F}[q(t)]$ is the Fourier transform of the Gaussian noise and $\delta(f)$ is the Dirac delta function.

The non-linearity introduces signals at frequencies other than those present in the input: those at $2F_1$ and $2F_2$ are denoted the harmonics and those at $F_1 + F_2$ and $F_2 - F_1$ are the intermodulation, or mixing, signals. Note that the signals resulting from the non-linearity are related in phase to those that generated them by relationships of the form $\phi_a + \phi_b - \phi_c = 0$, where ϕ_a , ϕ_b and ϕ_c are the constant phase differences associated with the three related components. This is quadratic phase coupling and offers a way of distinguishing signals at a particular frequency that are due to system non-linear behaviour from those which are not. The statistics of estimating the response due to mixing at $F_1 + F_2$ will be considered, analogous calculations are possible for the harmonics or the other mixing signal. Only components that contribute to $B(F_1, F_2)$ are of interest and so a reduced time-domain response is defined that contains only the information corresponding to the excitation frequencies, the intermodulation signal at $F_3 = F_1 + F_2$ and the noise $Q(t)$, and neglects all other terms in Eq. (9):

$$x(t) = S_1 \sin(2\pi F_1 t + \phi_1) + S_2 \sin(2\pi F_2 t + \phi_2) - S_3 \cos(2\pi F_3 t + \phi_3) + q(t). \tag{11}$$

Although S_3 and ϕ_3 are defined as independent variables for generality, for quadratic systems $S_3 = \beta S_1 S_2$ and $\phi_3 = \phi_1 + \phi_2$. In the reduced response $t = 0$ is selected such that $\phi_1 = \phi_2 = 0$ and hence $\phi_3 = 0$. The deterministic part of the signal is denoted $x^{(S)}(t) = S_1 \sin 2\pi F_1 t + S_2 \sin 2\pi F_2 t - S_3 \cos 2\pi(F_3)t$ and so the total response can be written more concisely as:

$$x(t) = x^{(S)}(t) + q(t). \tag{12}$$

The positive-frequency domain response can be written as:

$$\begin{aligned}
X(f) = \mathcal{F}[x(t)] &= X^{(S)}(f_n) + Q(f_n) \\
&= -i\frac{\alpha S_1}{2}\delta(F_1 - f)e^{i\phi_1} - i\frac{\alpha S_2}{2}\delta(F_2 - f)e^{i\phi_2} \\
&\quad - \frac{S_3}{2}\delta(F_3 - f)e^{i\phi_3} + Q(f)
\end{aligned} \tag{13}$$

3. Exploiting quadratic phase coupling

The bispectrum detects signals that are quadratically phase coupled (QPC) and suppresses those that are not, which is why it is of interest for identifying system non-linearity. When the expectation value over an ensemble of possible responses is considered only those frequency pairs where $\phi_1 + \phi_2 - \phi_3 = 0$ lead to constructive addition.

To more clearly demonstrate how quadratic phase coupling affects the bispectrum, consider a response as defined in Eq. (11), but without the noise term $q(t)$ (as previously $F_3 = F_1 + F_2$). M measurements each of length N and labelled k are considered:

$$x_k(t) = S_1 \sin(2\pi F_1 t + \phi_{1k}) + S_2 \sin(2\pi F_2 t + \phi_{2k}) - S_3 \cos(2\pi(F_3)t + \phi_{3k}) \quad (14)$$

The three components are related in frequency, and have phases ϕ_{1k} , ϕ_{2k} and ϕ_{3k} , which are to be specified. Using the average over M measurements to evaluate the expectation value operator in Eq. (2) approximates the bispectrum at F_1, F_2 as:

$$\begin{aligned} \hat{B}(F_1, F_2) &= \frac{1}{M} \sum_{k=1}^M X_k(F_1) X_k(F_2) X_k^*(F_3) \\ &= \frac{1}{8M} S_1 S_2 S_3 \sum_{k=1}^M \exp [i(\phi_{1k} + \phi_{2k} - \phi_{3k})] \end{aligned} \quad (15)$$

Consider the case where the phases of the excitations (ϕ_{1k} and ϕ_{2k}) are both randomly distributed and independent for each measurement: if the signal at S_3 is quadratically phase coupled with regard to the excitations then $\phi_{1k} + \phi_{2k} - \phi_{3k} = 0$ for all k and the estimated bispectrum goes to:

$$\hat{B}(F_1, F_2) = \frac{1}{8} S_1 S_2 S_3. \quad (16)$$

If the phase component at F_3 , ϕ_{3k} , is also randomly distributed with respect to ϕ_{1k} and ϕ_{2k} then the summation in Eq. (15) sums components randomly distributed in phase and so tends to zero as M increases leading to a bispectrum of zero. This allows detection of quadratically phase coupled responses (such as those produced by excitation of quadratic non-linear systems) while suppressing signals at the appropriate frequency, but with uncorrelated phase.

When sinusoidal excitations are used there are two practical approaches to probing non-linear systems that require some thought and care with regard to quadratic phase coupling: multiple measurements taken using the same excitation signal and the division of a single measurement into multiple records for averaging.

If the same excitation is used for each measurement then the phase of each excitation component is fixed: $\phi_{1k} = \phi_1$, $\phi_{2k} = \phi_2$ and Eq. (15) simplifies to:

$$B(F_1, F_2) = \frac{1}{8M} S_1 S_2 S_3 e^{i(\phi_1 + \phi_2)} \sum_{k=1}^M e^{-\phi_{3k}}. \quad (17)$$

If the third phase is randomly distributed then the summation will tend to zero, whereas a constant relative phase $\phi_{3k} = \phi_3$ will lead to a complex bispectrum of the amplitude

given by Eq. (16) and phase $\phi_1 + \phi_2 - \phi_3$. Although this allows detection of phase coupled systems (and suppression of signals which are not phase coupled) it should be noted that similar behaviour occurs if the frequency domain signal at F_3 is averaged:

$$\widehat{X}(F_1 + F_2) = \frac{1}{2} \frac{N}{M} S_3 \sum_{k=1}^M e^{-\phi_3 k}. \quad (18)$$

Therefore, in this case, the bispectrum does not provide any advantage, over direct averaging of the system response, in terms of suppressing non-phase-coupled systems.

To this point it has been assumed that each record constitutes a separate measurement, however for stochastic systems it is common to use a single time trace ($x(t_j)$) and divide it into K segments. For systems where the amplitude and phase at a given frequency varies with time, dividing a single record into K segments is equivalent of making K different measurements on the same system. It is not obvious however whether the same approach can be applied to systems where there are ongoing sinusoidal excitations. Consider a single record of the same form as that in Eq. (14). This record is then divided into K sections each of $n = N/K$ points, each record can be written:

$$\begin{aligned} x_k(t) &= S_1 \sin(2\pi F_1(t + k\Delta t) + \phi_1) + S_2 \sin(2\pi F_2(t + k\Delta t) + \phi_2) \\ &- S_3 \cos(2\pi(F_1 + F_2)(t + k\Delta t) + \phi_3). \end{aligned} \quad (19)$$

Δt is the length of each section ($\Delta t = \frac{n}{f_s}$). The corresponding Fourier transforms at the frequencies of interest are:

$$X_k(F_1) = \frac{1}{2} i S_1 e^{i(2\pi F_1 k \Delta t + \phi_1)}$$

$$X_k(F_2) = \frac{1}{2} i S_2 e^{i(2\pi F_2 k \Delta t + \phi_2)}$$

$$X_k(F_3) = -\frac{1}{2} S_3 e^{i(2\pi(F_1 + F_2)k \Delta t + \phi_3)} \quad (20)$$

$$(21)$$

Averaging over the segments gives

$$\begin{aligned} \widehat{B}(F_1, F_2) &= \frac{1}{M} \sum_{k=1}^M X(F_1) X(F_2) X^*(F_3) \\ &= \frac{1}{8M} S_1 S_2 S_3 e^{i(\phi_1 + \phi_2 - \phi_3)} \dots \end{aligned} \quad (22)$$

$$\begin{aligned} &\sum_{k=1}^M e^{i[2\pi F_1 k \Delta t + 2\pi F_2 k \Delta t - 2\pi(F_1 + F_2)k \Delta t]} \\ &= \frac{1}{8} S_1 S_2 S_3 e^{i(\phi_1 + \phi_2 - \phi_3)} \end{aligned} \quad (23)$$

So where the signals are quadratically phase coupled the bispectrum is real, but the magnitude of the bispectrum is the same regardless of the phase relation, making the detection of quadratically phase coupled systems difficult.

4. Statistical analysis of estimators

So far as application to detecting small non-linearities is concerned the quality of an estimator is determined by two things: the difference in magnitude of the estimated value in the presence of non-linearities from that of a linear system and how variable the estimate itself is. For an ideal measurement, the measured response should be zero in the absence of non-linearity, increase with increasing non-linearity and exhibit zero variance. These ideal cases only occur in the case of zero noise. In this section the expected values of the estimators of powerspectrum and bispectrum defined in section 2 are evaluated for the test signal in Eq. (11) (with $\phi_1 = \phi_2 = \phi_3 = 0$), along with their variances. Appropriate signal-to-noise ratios are defined to provide comparison of the different spectral methods. The results will be demonstrated with artificial (and hence well defined) data containing computationally generated Gaussian noise.

4.1. Defining signal-to-noise ratios

Comparison of the effectiveness of the methods for estimating the signals is most commonly achieved by looking at signal-to-noise ratios (SNRs) and this approach will be applied here. The definition of the signal-to-noise ratio is however complicated by the expected value of the bispectrum being zero for responses with only noise.

Let $\Phi(\beta, \sigma)$ denote either the powerspectrum or the bispectrum when applied to a response spectrum from a system with quadratic non-linearity β and Gaussian noise of variance σ^2 . The most straightforward signal-to-noise ratio is to compare the expected value for a non-linear signal with no noise, $E[\widehat{\Phi}(\beta, \sigma = 0)]$, to that for the case where there is noise and no non-linearity, $E[\widehat{\Phi}(\beta = 0, \sigma)]$. Hence we have an SNR:

$$\text{SNR}_1(\beta, \sigma) = \left(\frac{E[\widehat{\Phi}(\beta, \sigma = 0)]}{E[\widehat{\Phi}(\beta = 0, \sigma)]} \right)^{1/a}. \quad (24)$$

The root power, a , is set to ensure that the SNR is proportional to the parameter of interest, here β or equivalently S_3 . Hence we set $a = 2$ for the powerspectrum and $a = 1$ for the bispectrum. This definition of the SNR loosely represents the expected average SNR from multiple measurements, however it becomes problematic for the bispectrum as the expected value goes to zero when there is no non-linearity (i.e $\beta = 0$) and so this SNR tends to infinity in this case.

A second SNR is defined, representing the worst-case SNR likely to be encountered in any particular measurement. It is assumed that the worst case consists of a low outlier being measured for the signal and a high outlier for the noise value. Taking the outliers as a number, b , of standard deviations from the expected value yields

$$\text{SNR}_2(\beta, \sigma) = \left(\frac{E[\widehat{\Phi}(\beta, \sigma)] - b\sqrt{\text{Var}(\widehat{\Phi}(\beta, \sigma))}}{E[\widehat{\Phi}(0, \sigma)] + b\sqrt{\text{Var}(\widehat{\Phi}(0, \sigma))}} \right)^{1/a}. \quad (25)$$

As an indicator of the values of b that are appropriate: for normally distributed values, $b = 1$ would indicate that 84.1% of measurements lie above the expected value minus b standard deviations, and $b = 2$ would lead to 97.7% lying in that region.

In order to quantify these SNRs and assess the effectiveness of the techniques in detecting the signal due to a small quadratic non-linearity the expected value and variance of each estimator are evaluated. That is analytic expressions of $E[\widehat{B}(F_1, F_2)]$, $E[\widehat{P}(F_3)]$, $E[\widehat{P}'(F_3)]$, $\text{Var}[\widehat{B}(F_1, F_2)]$, $\text{Var}[\widehat{P}(F_3)]$ and $\text{Var}[\widehat{P}'(F_3)]$ are sought.

The variance of a general spectrum estimate $\widehat{\Phi}(S_3, \sigma) = \widehat{\Phi}(S_1, S_2, S_3, \sigma, M, N)$, where $\widehat{\Phi}$ can be \widehat{B} , \widehat{P} or \widehat{P}' , is given by

$$\text{Var}[\widehat{\Phi}(S_3, \sigma)] = \sigma_{\widehat{\Phi}}^2 = E[\widehat{\Phi}(S_3, \sigma)\widehat{\Phi}^*(S_3, \sigma)] - E[\widehat{\Phi}(S_3, \sigma)]E[\widehat{\Phi}^*(S_3, \sigma)], \quad (26)$$

which also defines the standard deviation $\sigma_{\widehat{\Phi}}$ of the function.

4.2. Numerical model

In order to illustrate the behaviour of the estimators artificial data with Gaussian white noise added is generated for a sample system, defined by Eq. (7) and excited the input defined by Eq. (8). Parameters are selected to give behaviour of the type observed in ultrasonic intermodulation experiments of the type performed by Hillis et al. [11, 31]. Fig. 2 shows the time domain and frequency domain responses with parameters $\alpha = 1$ and $\beta = 0.01$, excited with amplitudes $S_1 = S_2 = 1$ at $F_1 = 300\text{kHz}$ and $F_2 = 400\text{kHz}$. As the system is quadratic $S_3 = \beta S_1 S_2 = 0.01$ at $F_3 = 700\text{kHz}$. The system is contaminated with Gaussian noise of variance $\sigma^2 = 1$. The peak in the signal at F_3 is expected to be $|X^{(S)}(F_3)| = \frac{S_3}{2}$ based on Eqs. (10) and (35).

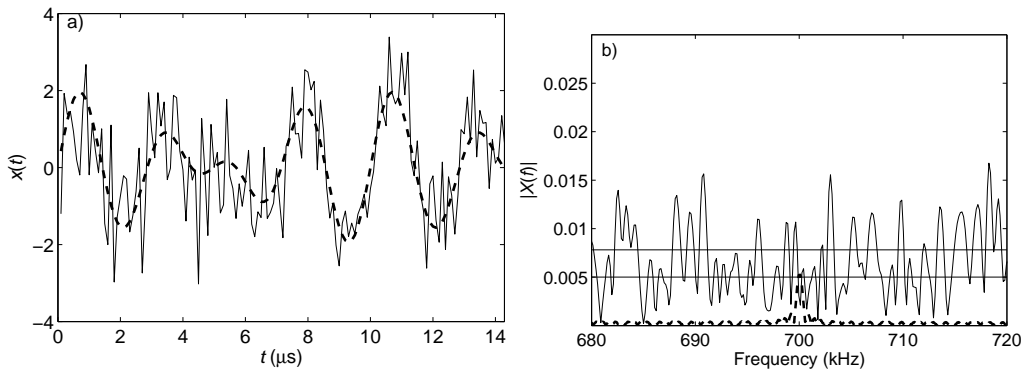


Figure 2: Artificial data generated for a quadratic non-linear system (with $\alpha = 1$ and $\beta = 0.01$), excited at $F_1 = 300\text{kHz}$ and $F_2 = 400\text{kHz}$ with additive Gaussian noise of variance $\sigma^2 = 1$. (a) the time domain response, (b) the powerspectrum in the region of F_3 . In each case the solid line is the response including noise and the dashed line the signal without noise added. In (b) the lower horizontal line marks the expected value of the signal at $F_3 = S_3/2$, and the upper horizontal line shows the standard deviation of the noise in the frequency domain, $\sigma/N^{1/2}$ (see Eq. 35).

4.3. Statistics of noise in the frequency domain

Having defined the system and the statistical measures of interest, the analysis required to evaluate those values is performed. First the statistics of the noise in the

frequency domain are evaluated as these are used repeatedly in the calculation of the expectation values and variances of the estimators.

The discrete Fourier transform (DFT), which is used to transform from the time to the frequency domain, is given by

$$A(f_n) = \frac{1}{N} \sum_{j=0}^{N-1} a(t_j) \exp(-i2\pi nj/N) \quad (27)$$

assessed at $f_n = n/T$ and $n = 0 \dots N - 1$.

The noise is assumed to be zero-mean and Gaussian, so that the probability of the noise at a particular time, t , lying in the infinitesimal range $q(t), q(t) + dq$ is:

$$\Pr[q(t)]\delta q = \frac{1}{\sigma\sqrt{2\pi}} \exp\left\{-\frac{q^2(t)}{2\sigma^2}\right\} \delta q \quad (28)$$

where σ^2 is the variance of the noise and $\Pr[\dots]$ the probability density. The expected value of a function of x , $f(x)$, is defined as

$$\mathbb{E}[f(x)] = \int_{-\infty}^{\infty} \Pr[x] f(x) dx. \quad (29)$$

$\mathbb{E}[q(t)] = 0$ as $q(t)$ is defined as zero mean. When calculating the expected values and variances of the spectra various powers of $Q(f)$ occur, which in turn depend on powers of $q(t)$. From Eqs. (28) and (29) odd powers of the noise have a zero expected value and utilizing the integral [35]

$$\int_{-\infty}^{+\infty} x^{2n} \exp[-ax^2] dx = \frac{(2n-1)!!}{2^{n+1}a^n} \sqrt{\frac{\pi}{a}} \quad (30)$$

where !! indicates the double factorial, even powers give

$$\begin{aligned} \mathbb{E}[q^{2n}(t)] &= \int_{-\infty}^{+\infty} q^{2n}(t) \frac{1}{\sigma\sqrt{2\pi}} \exp\left\{-\frac{q^2(t)}{2\sigma^2}\right\} dq \\ &= (2n-1)!!\sigma^{2n}, \end{aligned} \quad (31)$$

where n is any positive integer. Of particular use in later analysis are the cases where $n = 1$ and $n = 2$: $\mathbb{E}[q^2(t)] = \sigma^2$, which (by virtue of the noise being zero mean) returns the noise variance, and $\mathbb{E}[q^4(t)] = 3\sigma^4$.

The expected value of the noise in the frequency domain, using Eq. (27) is

$$\mathbb{E}[Q(f)] = \mathbb{E}\left[\frac{1}{N} \sum_{j=0}^{N-1} q(t_j) e^{(-i2\pi nj/N)}\right] = \frac{1}{N} \sum_{j=0}^{N-1} e^{(-i2\pi nj/N)} \mathbb{E}[q(t_j)] = 0 \quad (32)$$

where the subscript for the discrete frequency has been dropped from the left hand side, but it is assumed that f fulfils $f = n/T$ where n is an integer.

When it comes to evaluating the expected values of products of the Fourier transform of the noise and the conjugate of the noise it is useful to bear in mind the expected value of the product of independently distributed variables is equal to product of the expected values of those variables:

$$\mathbb{E}[x_1 x_2] = \mathbb{E}[x_1] \mathbb{E}[x_2], \quad \mathbb{E}[x_1 x_2 x_3] = \mathbb{E}[x_1] \mathbb{E}[x_2] \mathbb{E}[x_3]. \quad (33)$$

Hence the expected value of the product of the frequency domain noise with the conjugate of the noise, $\mathbb{E}[Q_j(f_1)Q_k(f_2)^*]$, is non-zero only if $f_1 = f_2$ and $j = k$. If this criteria is met:

$$\begin{aligned} \mathbb{E}[Q_j(f_1)Q_j(f_1)^*] &= \mathbb{E}\left[\frac{1}{N}\sum_{l=1}^N q_j(t_l)e^{(-i2\pi n l/N)}\frac{1}{N}\sum_{m=1}^N q_j^*(t_m)e^{(i2\pi n m/N)}\right] \\ &= \frac{1}{N^2}\sum_{l,m} e^{(-i2\pi n(m-l))}\mathbb{E}[q_j(t_l)q_j(t_m)]. \end{aligned} \quad (34)$$

As $q(t)$ consists of independent randomly-distributed zero-mean values, the expectation value is zero when $m \neq l$, and the value for $m = l$ is $\mathbb{E}[q(t)q(t)] = \sigma^2$ the summation is zero for all indices (l, m) except the N values where $l = m$. For those cases the power of the exponential term is zero (the exponential term is unity) and so

$$\begin{aligned} \mathbb{E}[Q_i(f_1)Q_j^*(f_2)] &= \frac{1}{N}\sigma^2 \quad \text{for } i = j \text{ and } f_1 = f_2. \\ &= 0 \quad \text{for } i \neq j \text{ or } f_1 \neq f_2. \end{aligned} \quad (35)$$

If the conjugate is not taken for the second term the summation goes to zero (see Appendix A.1), even for $i = j$, giving

$$\mathbb{E}[Q_i(f)Q_j(f)] = 0 \quad \text{for all } i, j. \quad (36)$$

For the product of four noise terms, $\mathbb{E}[Q_i(f)Q_j^*(f)Q_k^*(f)Q_l(f)]$, similar calculations to Eq. (34) apply (shown in Appendix A.2) leading to:

$$\begin{aligned} \mathbb{E}[Q_i(f)Q_j^*(f)Q_k^*(f)Q_l(f)] &= \frac{2}{N^2}\sigma^4 \quad \text{for } i = j = k = l \\ &= \frac{1}{N^2}\sigma^4 \quad \text{for } i = j \neq k = l \\ &= \frac{1}{N^2}\sigma^4 \quad \text{for } i = k \neq j = l \\ &= 0 \quad \text{all others,} \end{aligned} \quad (37)$$

4.4. Expected values and variances of estimators

The Powerspectrum. Applying the powerspectrum estimator defined in Eq. (4) to the test response Eq. (11), and evaluating the expected value at F_3 using Eqs. (33) and (35):

$$\begin{aligned} \mathbb{E}\left[\widehat{P}(F_1 + F_2)\right] &= \frac{1}{M}\sum_{i=1}^M \left\{ \mathbb{E}[X_i(F_3)X_i^*(F_3)] \right\} \\ &= \frac{1}{M}\sum_{i=1}^M \left\{ \mathbb{E}\left[\left(X^{(S)}(F_3)X^{(S)*}(F_3) + Q_i(F_3)Q_i^*(F_3)\right)\right] \right\} \\ &= \frac{S_3^2}{4} + \frac{1}{N}\sigma^2. \end{aligned} \quad (38)$$

Note that the powerspectrum includes a noise term. This noise depends on the noise in the initial response and the number of points used for the Fourier transform; averaging does not reduce the noise contribution. The expected value of the conjugate product of the estimator, required for the variance, is evaluated using Eqs. (33), (35), (36) and (37):

$$\mathbb{E} \left[\widehat{P}(F_3) \widehat{P}^*(F_3) \right] = \mathbb{E} \left[\frac{1}{M^2} \sum_{j,k=1}^M \left\{ X_j(F_3) X_j^*(F_3) X_k(F_3) X_k^*(F_3) \right\} \right] \quad (39)$$

Along with Eq. (38) this gives the variance:

$$\text{Var} \left[\widehat{P}(F_3) \right] = \mathbb{E} \left[\widehat{P}(F_3) \widehat{P}^*(F_3) \right] - \mathbb{E} \left[\widehat{P}(F_3) \right] \mathbb{E} \left[\widehat{P}^*(F_3) \right] = \frac{\sigma^4}{MN^2} + \frac{S_3^2 \sigma^2}{2MN} \quad (40)$$

The Powerspectrum of the Average Response. The expected value of powerspectrum of the average response (defined in Eq. (5)) at F_3 , can be calculated using Eqs. (33), (35) and (36):

$$\begin{aligned} \mathbb{E}[\widehat{P}'(F_3)] &= \frac{1}{M^2} \sum_{i,j=1}^M \left\{ \mathbb{E} \left[\left(X^{(S)}(F_3) + Q_i(F_3) \right) \left(X^{(S)*}(F_3) + Q_j^*(F_3) \right) \right] \right\} \\ &= \frac{S_3^2}{4} + \frac{1}{MN} \sigma^2. \end{aligned} \quad (41)$$

This approach to the averaging leads to a noise term that reduces with number of averages, M .

The variance of this estimate requires the calculation of $\mathbb{E} \left[\widehat{P}'(F) \widehat{P}'^*(F) \right]$:

$$\begin{aligned} \mathbb{E}[\widehat{P}'(F_3) \widehat{P}'^*(F_3)] &= \mathbb{E} \left[\frac{1}{M^4} \sum_{i,j,k,l=1}^M \left\{ \left(X^{(S)}(F_3) + Q_i(F_3) \right) \right. \right. \\ &\quad \times \left(X^{(S)*}(F_3) + Q_j^*(F_3) \right) \left(X^{(S)}(F_3) + Q_k(F_3) \right) \\ &\quad \left. \left. \times \left(X^{(S)}(F_3) + Q_l(F_3) \right) \right\} \right] \\ &= \frac{1}{M^4} \sum_{i,j,k,l=1}^M \left\{ X^{(S)}(F_3) X^{(S)*}(F_3) X^{(S)*}(F_3) X^{(S)}(F_3) \right. \\ &\quad + X^{(S)}(F_3) X^{(S)*}(F_3) (\mathbb{E}[Q_k^*(F_3) Q_l(F_3)]) \\ &\quad + \mathbb{E}[Q_l^*(F_3) Q_j(F_3)] + \mathbb{E}[Q_i^*(F_3) Q_k(F_3)] \\ &\quad + \mathbb{E}[Q_i^*(F_3) Q_j(F_3)] \\ &\quad \left. + \mathbb{E}[Q_i(F_3) Q_j^*(F_3) Q_k^*(F_3) Q_l(F_3)] \right\} \end{aligned} \quad (42)$$

The results of the summations are derived in Appendix B, and applied to Eq. (42) giving

$$\mathbb{E}[\widehat{P}'(F_3) \widehat{P}'^*(F_3)] = \frac{S_3^4}{16} + \frac{1}{M^3 N^2} \sigma^4 + \frac{2}{M^2 N^2} \sigma^4 + \frac{1}{MN} S_3^2 \sigma^2 \quad (43)$$

Combining Eqs. (41) and (43) gives the variance:

$$\text{Var} \left[\widehat{P}'(F_3) \right] = \frac{\sigma^4}{M^2 N^2} + \frac{S_3^2 \sigma^2}{2MN} \quad (44)$$

The Bispectrum. The expected value of the bispectrum estimator at F_1, F_2 is given by applying the estimator defined in Eq. (6) to the test response in Eq. (11) and evaluating the expected value.

$$\text{E} \left[\widehat{B}(F_1, F_2) \right] = \text{E} \left[\frac{1}{M} \sum_{i=1}^M X_i(F_1) X_i(F_2) X_i^*(F_3) \right] \quad (45)$$

From Eq. (13) and making use of Eqs. (33), (35) and (36), gives

$$\begin{aligned} \text{E} \left[\widehat{B}(F_1, F_2) \right] &= \text{E} \left[\frac{1}{M} \sum_{i=1}^M \left\{ \left(X^{(S)}(F_1) + Q_i(F_1) \right) \right. \right. \\ &\quad \left. \left. \times \left(X^{(S)}(F_2) + Q_i(F_2) \right) \left(X^{(S)*}(F_3) + Q_i^*(F_3) \right) \right\} \right] \\ &= \frac{1}{M} \sum_{k=1}^M \left\{ X^{(S)}(F_1) X^{(S)}(F_2) X^{(S)*}(F_3) \right. \\ &\quad + \text{E} [Q_i(F_2)] X^{(S)}(F_1) X^{(S)*}(F_3) \\ &\quad + \text{E} [Q_i(F_1)] X^{(S)}(F_2) X^{(S)*}(F_3) \\ &\quad + \text{E} [Q_i(F_1) Q_i(F_2)] X^{(S)*}(F_3) \\ &\quad + X^{(S)}(F_1) X^{(S)}(F_2) \text{E} [Q_i^*(F_3)] \\ &\quad \left. + \text{E} [Q_i(F_1) Q_i(F_2) Q_i^*(F_3)] \right\} \\ &= \frac{1}{M} \sum_{k=1}^M \left\{ X^{(S)}(F_1) X^{(S)}(F_2) X^{(S)*}(F_3) \right\} \\ &= \frac{S_1 S_2 S_3}{8}. \end{aligned} \quad (46)$$

Note that the final step contains no noise terms and so Eqs. 15 and 16 (where noise was ignored) can be used. The expected value of the estimator is proportional to the signal, S_3 , at the mixing frequency (and so to β) and tends to zero if there is no mixing.

The variance of the bispectrum estimator is

$$\text{Var} \left[\widehat{B}(F_1, F_2) \right] = \text{E} \left[\widehat{B}(F_1, F_2) \widehat{B}^*(F_1, F_2) \right] - \text{E} \left[\widehat{B}(F_1, F_2) \right] \text{E} \left[\widehat{B}^*(F_1, F_2) \right] \quad (47)$$

where $\text{E} \left[\widehat{B}(F_1, F_2) \right]$ is given in Eq. (46). $\text{E} \left[\widehat{B}(F_1, F_2) \widehat{B}^*(F_1, F_2) \right]$ is evaluated using

Measure	Amplitude (no noise)	Amplitude (with noise)	Variance
Powerspectrum, $\widehat{P}(F_3)$	$\frac{S_3^2}{4}$	$\frac{S_3^2}{4} + \frac{1}{N}\sigma^2$	$\frac{\sigma^4}{MN^2} + \frac{S_3^2\sigma^2}{2MN}$
Powerspectrum of Average Response, $\widehat{P}'(F_3)$	$\frac{S_3^2}{4}$	$\frac{S_3^2}{4} + \frac{1}{MN}\sigma^2$	$\frac{\sigma^4}{M^2N^2} + \frac{S_3^2\sigma^2}{2MN}$
Bispectrum, $\widehat{B}(F_1, F_2)$	$\frac{S_1S_2S_3}{8}$	$\frac{S_1S_2S_3}{8}$	$\frac{S_1^2S_2^2\sigma^2}{16NM} + \frac{S_1^2S_3^2\sigma^2}{16NM} + \frac{S_2^2S_3^2\sigma^2}{16NM}$ $+ \frac{S_1^2\sigma^4}{4N^2M} + \frac{S_2^2\sigma^4}{4N^2M} + \frac{S_3^2\sigma^4}{4N^2M}$ $+ \frac{1}{N^3M}\sigma^6$

Table 1: Summary of expected values of estimators and their variances.

Eqs. (13), (33) and (35) to give the variance.

$$\begin{aligned}
\mathbb{E} \left[\widehat{B}(F_1, F_2) \widehat{B}^*(F_1, F_2) \right] &= \frac{1}{M^2} \sum_{j,k=1}^M \left\{ \mathbb{E} [X_j(F_1) X_k^*(F_1)] \right. \\
&\quad \left. \times \mathbb{E} [X_j(F_2) X_k^*(F_2)] \mathbb{E} [X_j^*(F_3) X_k^*(F_1)] \right\} \\
&= \frac{1}{M^2} \left[M \left(\frac{S_1^2}{4} + \frac{1}{N} \sigma^2 \right) \right. \\
&\quad \left. \times \left(\frac{S_2^2}{4} + \frac{1}{N} \sigma^2 \right) \left(\frac{S_3^2}{4} + \frac{1}{N} \sigma^2 \right) \right] \\
&\quad + M(M-1) \frac{S_1^2 S_2^2 S_3^2}{64} \\
&= \frac{S_1^2 S_2^2 S_3^2}{64} + \frac{S_1^2 S_2^2 \sigma^2}{16NM} + \frac{S_1^2 S_3^2 \sigma^2}{16NM} + \frac{S_2^2 S_3^2 \sigma^2}{16NM} \\
&\quad + \frac{S_1^2 \sigma^4}{4N^2M} + \frac{S_2^2 \sigma^4}{4N^2M} + \frac{S_3^2 \sigma^4}{4N^2M} + \frac{1}{N^3M} \sigma^6. \quad (48)
\end{aligned}$$

The resulting variance in the bispectrum at the intermodulation frequency pair is

$$\text{Var} \left[\widehat{B}(F_1, F_2) \right] = \frac{\sigma^2}{NM} \left(\frac{S_1^2 S_2^2}{16} + \frac{S_1^2 S_3^2}{16} + \frac{S_2^2 S_3^2}{16} + \frac{S_1^2 \sigma^2}{4N} + \frac{S_2^2 \sigma^2}{4N} + \frac{S_3^2 \sigma^2}{4N} + \frac{1}{N^2} \sigma^4 \right) \quad (49)$$

5. Comparison of estimators

Having calculated the expected values of the estimators and their variances, this section compares the analytical results to numerical values, and evaluates the signal-to-noise ratios developed in section 4.1.

5.1. Expected values and variance

Table 1 summarizes the values evaluated for the estimators of the powerspectrum and bispectrum. The behaviour of these values is illustrated in Figs. 3 (a) and (b), which

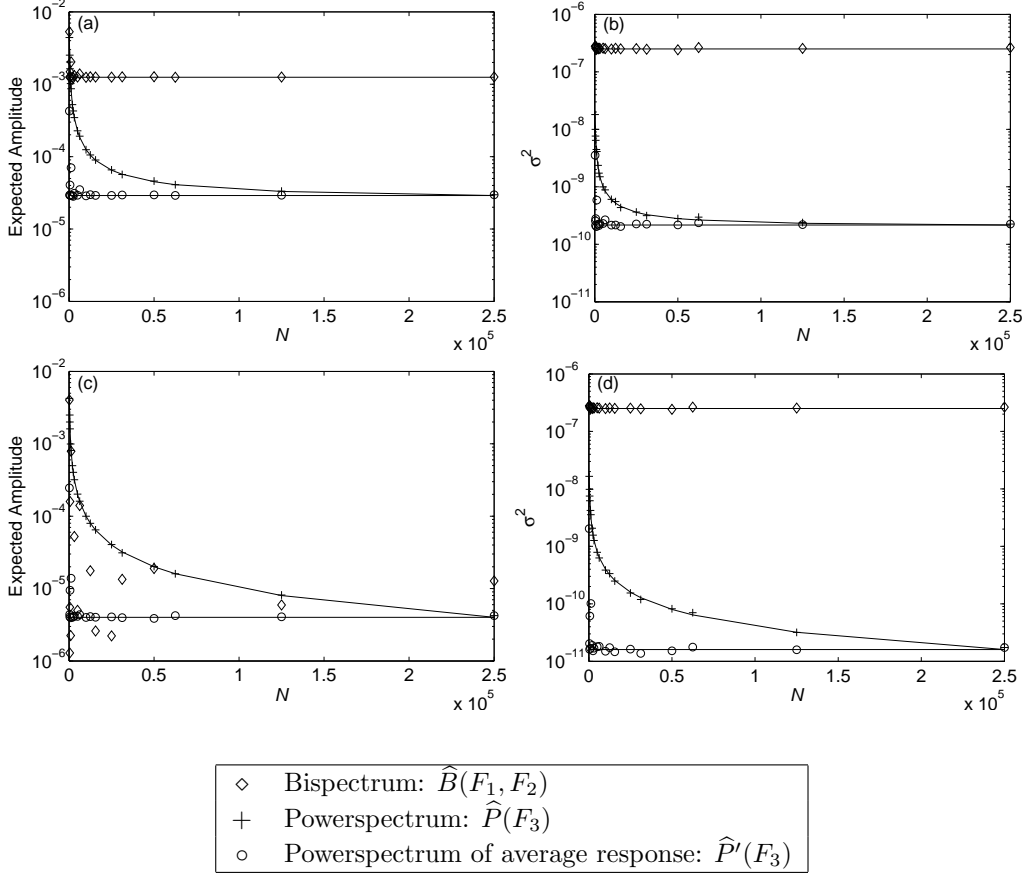


Figure 3: (a) The expected value of the estimated frequency domain response at the mixing frequency F_3 due to non-linearity for a quadratic non-linear system (with $\alpha = 1$ and $\beta = 0.01$), excited at $F_1 = 300\text{kHz}$ and $F_2 = 400\text{kHz}$ with additive Gaussian noise of variance $\sigma^2 = 1$. (b) The variance of the estimate. (c) The expected value at F_3 in the absence of non-linearity ($\alpha = 1$ and $\beta = 0$). (d) The variance of the estimates shown in (c). Numerical data points are as defined in legend and solid lines represent analytical results as summarized in Table 1

show how the estimated value and its variance varies for increasing record length, N , with the total number of data points, $NM = 250000$, held constant. The system was as described in section 4.2 and the expectation value of each estimator was determined as the average value of the estimator over $N_R = 1000$ repetitions of the test. In each case the data from the model closely follows the analytical results, except at relatively low (<1000) values of N . In this region leakage, due to windowing, of the large components at F_1 and F_2 becomes appreciable at F_3 and so increases the expected value over that evaluated analytically. The variance of the estimators, for both numerical and analytical results, are (barring the leakage effect at low N) as predicted.

In addition to how well, and how consistently, the estimators characterize the signal due to non-linearity it is useful to know how large the measured response is for cases where

there is no non-linearity. Fig. 3 (c) and (d) show the result of repeating the calculations shown in Fig. 3 (a) and (b) for a system with $\beta = 0$, and hence $S_3 = 0$. In both the powerspectrum and the powerspectrum of the average response the numerical results follow the values calculated in section 4.2. However for the bispectrum the expected value, given by Eq. (46), tends to zero as S_3 tends to zero. Also the bispectrum, unlike the power spectrum, is not bounded by zero; negative values are possible and for $S_3 = 0$ likely. For this reason the absolute value of the expected bispectrum is plotted in Fig. 3 to allow comparison with the powerspectrum values. As the expected value of the measurement is expected to be zero the effect of the variation of the test results dominates. Although this indicates a failing in the use of averaging over a number of repetitions to approximate the expected value (and the values could be reduced by increasing N_R) it does highlight that it is not sufficient to consider only the expected value of the estimator when considering its efficiency in producing estimates. This distinction is taken up further in section 5.2 where appropriate signal-to-noise ratios are developed and used to compare the techniques.

From Fig. 3 it can be seen that for a given total number of points NM the statistics of the powerspectrum of the average response are not dependent on how these points are divided, this follows from M and N only appearing as MN or a power thereof in the expected values and variance as shown in table 1. The expected value of the response for the powerspectrum is unaffected by averaging (M does not appear in the noise term of the expected value), so the noise term is minimized by maximizing N , which can be achieved by setting $M = 1$. Similarly the variance of the powerspectrum estimator is minimized when N is minimised. For $M = 1$ the powerspectrum coincides with the powerspectrum of the average response, for all other combinations of M and N the average response method is superior. It is also the case that, although the expectation value of the actual estimate provided by the bispectrum is not dependent on the split of data, the variance is minimized for $M = 1$.

Fig. 4 shows the estimated powerspectra and bispectra respectively for 100 different values of S_3 regularly distributed between zero and 0.05 calculated for $N = 250000$ and $M = 1$. The expected value of the estimators are plotted along with these values plus and minus twice the standard deviations. It can be seen that the majority of values (96 and 90 for the bispectrum and powerspectrum respectively) lie within the bounds of these lines. Also shown, for comparison are the estimates obtained for $S_3 = 0$ for each data set, along with the associated estimates and bounds. The lower of the line used to determine the bounds of likely individual measurement ($E[\widehat{\Phi}(\beta, \sigma)] - 2\sigma_{\Phi}(\beta, \sigma)$) and the line marking the upper bound of the likely individual measurement for a linear system with the same excitation ($E[\widehat{\Phi}(\beta = 0, \sigma)] + 2\sigma_{\Phi}(\beta = 0, \sigma)$) contain the majority of measured values and it would be expected that where the $E[\widehat{\Phi}(\beta, \sigma)] - 2\sigma_{\Phi}(\beta, \sigma)$ is significantly greater than $E[\widehat{\Phi}(\beta = 0, \sigma)] + 2\sigma_{\Phi}(\beta = 0, \sigma)$ then the two systems will be clearly distinguished by a single measurement. This corresponds to the situation evaluated by SNR_2 defined in Eq. 25 for $b = 2$.

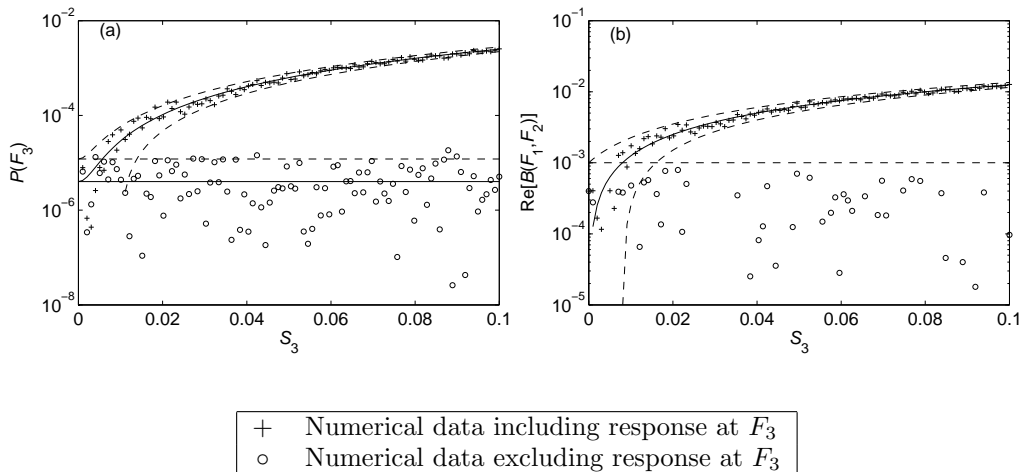


Figure 4: Estimates of (a) powerspectrum of average response and (b) bispectrum for system with $S_1 = S_2 = 1$ and S_3 varied from zero to 0.1 and white noise of variance $\sigma^2 = 1$ added. Spectra were estimated using $N = 250000$ and $M = 1$. The expected value (evaluated from Eqs. (41) and (46) respectively) is plotted as a solid line in each case and the confidence bounds given by the expected value plus or minus two standard deviations (from Eqs. (44) and (49) respectively) are shown as dashed lines.

5.2. Signal-to-noise ratios

Given the estimated value of the average response powerspectrum estimator, Eq. (41), the signal-to-noise ratio defined in Eq. (24) is

$$\begin{aligned}
 \text{SNR}_1^{(P')}(\beta, \sigma) &= \sqrt{\frac{\text{E}[\widehat{P}'^{(S)}(F_3)]}{\text{E}[\widehat{P}'^{(N)}(F_3)]}} \\
 &= \frac{S_3}{2\sigma} \sqrt{MN} = \frac{\beta S_1 S_2}{2\sigma} \sqrt{MN} = \gamma
 \end{aligned} \tag{50}$$

(S) indicates estimation applied to signals without noise and (N) indicates estimator applied to noise only. Eq. (50) also provides the physical meaning of the parameter γ which is used to simplify later comparisons. Note that for a given total number of data points, NM , this SNR is the same regardless of how they are divided between length of measurement and number of averages. The equivalent SNR for the average powerspectrum (using Eq. (38)) is

$$\text{SNR}_1^{(P)}(\beta, \sigma) = \frac{\text{SNR}_{(1)}^{(P')}(\beta, \sigma)}{\sqrt{M}} \tag{51}$$

and so the powerspectrum of the average response is superior, apart from the case $M = 1$ where the two are the same. The same is true of the variances given in Eqs. (40) and (44) (as seen in Fig. 3) indicating that the powerspectrum of the average response is the better estimate of the two therefore it is this estimator that is compared to the bispectrum.

As the expected value of the estimated bispectrum is zero where there is no noise the SNR defined in Eq. (24) tends to infinity and so the second SNR, which takes into account the worst case values, is considered using Eq. (25):

$$\begin{aligned}
\text{SNR}_2^{(P')} &= \sqrt{\frac{\frac{S_3^2}{4} + \frac{1}{MN}\sigma^2 - b\sqrt{\frac{1}{(NM)^2}\sigma^4 + \frac{1}{2MN}S_3^2\sigma^2}}{\frac{1}{MN}\sigma^2 + b\frac{1}{MN}\sigma^2}} \\
&= \frac{S_3}{2\sigma}\sqrt{\frac{MN}{1+b}}\sqrt{1 + \frac{4}{MN}\frac{\sigma^2}{S_3^2} - b\sqrt{\frac{16}{(MN)^2}\frac{\sigma^4}{S_3^4} + \frac{8}{MN}\frac{\sigma^2}{S_3^2}}} \\
&= \frac{\gamma}{\sqrt{1+b}}\sqrt{1 + \frac{1}{\gamma^2} - b\sqrt{\frac{2}{\gamma^2} + \frac{1}{\gamma^4}}} \tag{52}
\end{aligned}$$

Applying the definition in Eq. (25) to the bispectrum gives:

$$\begin{aligned}
\text{SNR}_2^{(B)} &= \frac{\frac{S_1 S_2 S_3}{8} - b\sqrt{\frac{\sigma^2}{NM}\left(\frac{S_1^2 S_2^2}{16} + \frac{S_1^2 S_3^2}{16} + \frac{S_2^2 S_3^2}{16} + \frac{S_1^2 \sigma^2}{4N} + \frac{S_2^2 \sigma^2}{4N} + \frac{S_3^2 \sigma^2}{4N} + \frac{1}{N^2}\sigma^4\right)}}{b\sqrt{\frac{\sigma^2}{NM}\left(\frac{S_1^2 S_2^2}{16} + \frac{S_1^2 \sigma^2}{4N} + \frac{S_2^2 \sigma^2}{4N} + \frac{1}{N^2}\sigma^4\right)}} \\
&= \frac{S_3}{2\sigma}\frac{\sqrt{MN}}{b} \\
&\quad \times \left(\frac{\frac{S_1 S_2}{4} - \frac{2\sigma}{S_3}\frac{b}{\sqrt{MN}}\sqrt{\frac{S_1^2 S_2^2 + S_1^2 S_3^2 + S_2^2 S_3^2}{16} + \frac{S_1^2 \sigma^2 + S_2^2 \sigma^2 + S_3^2 \sigma^2}{4N} + \frac{1}{N^2}\sigma^4}}{\sqrt{\frac{S_1^2 S_2^2}{16} + \frac{S_1^2 \sigma^2}{4N} + \frac{S_2^2 \sigma^2}{4N} + \frac{1}{N^2}\sigma^4}} \right) \tag{53}
\end{aligned}$$

For the case where the excitation amplitudes are the same, $S_1 = S_2 = S$, Eq. (53) simplifies to

$$\text{SNR}_2^{(B)} = \frac{\frac{\gamma}{b} - \sqrt{\left(1 + \frac{\beta^2 S^2 M}{\gamma^2}\right)^2 + \beta^2 S^2 \left(2 + \frac{\beta^2 S^2 M}{\gamma^2}\right)}}{1 + \frac{\beta^2 S^2 M}{\gamma^2}}. \tag{54}$$

By inspection, $\text{SNR}_2^{(B)}$ is maximized when M is minimized and therefore equal to unity. The limiting SNR_2 for a noisy and weakly non-linear system is now considered, as this is the regime where the performance of the bispectrum relative to the powerspectrum is of particular interest. A noisy system implies that the SNR of the powerspectrum at the mixing frequency, $\text{SNR}_1^{(P')}$, is close to unity, hence $\gamma \approx 1$. A weakly non-linear system implies that $S_3 \ll S$, which since $S_3 = \beta S$ gives $\beta S \ll 1$. The combination of these assumptions ($M = 1$, $\gamma \approx 1$ and $\beta S \ll 1$) enables Eq. (54) to be approximated to:

$$\text{SNR}_2^{(B)} \approx \frac{\gamma}{b} - 1 \tag{55}$$

Numerically this has been found to be a good approximation to Eq. (54) for values of β up to 0.1. The approximated $\text{SNR}_2^{(B)}$ given by Eq. (55) is a function of b and γ only and so can be compared directly to the $\text{SNR}_2^{(P')}$ given by Eq. (52).

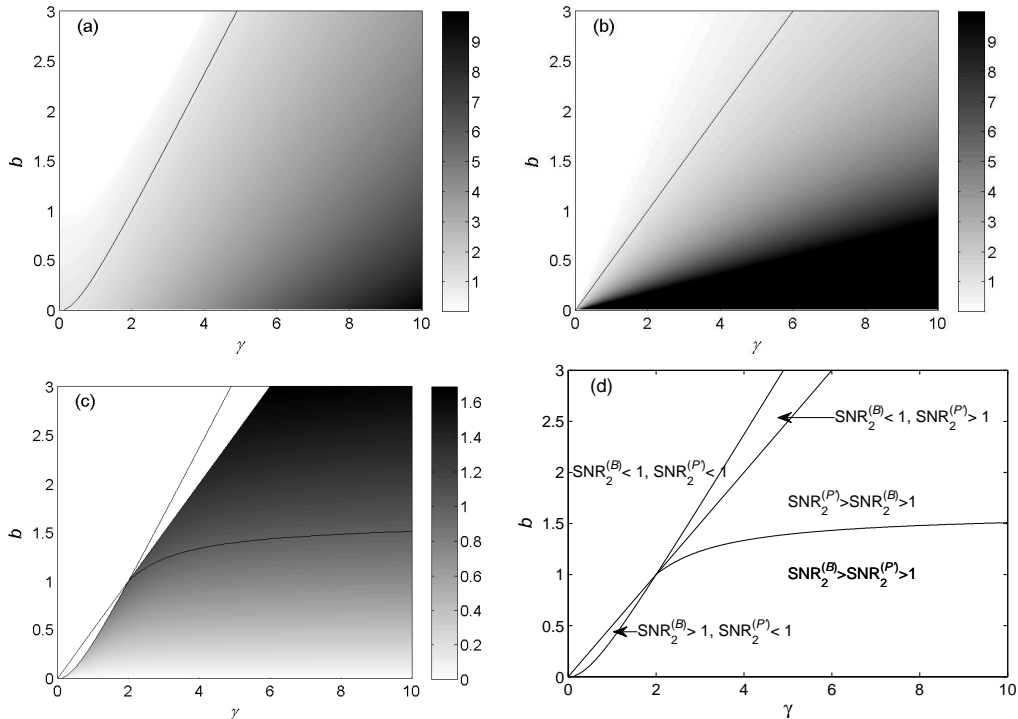


Figure 5: Comparison of $\text{SNR}_2^{(P')}$, and $\text{SNR}_2^{(B)}$ evaluated using Eqs. (52) and (55) respectively. (a) The value of $\text{SNR}_2^{(P')}$ with the line where $\text{SNR}_2^{(P')}=1$ marked. (b) The value of $\text{SNR}_2^{(B)}$ with the line where $\text{SNR}_2^{(B)}=1$ marked. (c) The ratio $\text{SNR}_2^{(P')}/\text{SNR}_2^{(B)}$ with the line where $\text{SNR}_2^{(B)} = \text{SNR}_2^{(P')}$ marked in addition to the two $\text{SNR}_2^{(\phi)} = 1$ lines. (d) The three lines shown in plot (c) and the regions they define according to the SNR relationships.

The parameter γ defined in Eq. 50 encapsulates the signal, noise and quantity of data. The parameter b is the number of standard deviations used to determine the bounds of a measurements probability distribution when calculating SNR_2 and so determines the confidence with which a given measurement can distinguish between a linear system and a non-linear system defined by γ . Of interest are the values of γ for a given b that give SNR_2 greater than unity (indicating that the signal can be differentiated from noise with the confidence associated with the specified value of b) and the ratio of the SNRs. Fig. 5 shows the variation of SNR with γ and b for both the powerspectrum, evaluated from Eq. 52, and the bispectrum, evaluated from Eq. 55, (Fig. 5 (a) and (b) respectively) and the ratio thereof (Fig. 5c)). Fig. 5(d) identifies resulting regions of interest in the b, γ plane. In each case the powerspectrum outperforms the bispectrum except where the parameter b is of the order of 1 or less. Equating the two SNRs and setting γ large enough to ignore $1/\gamma$ terms gives $b = 1.618$ (giving a 94.7% confidence) as the value at which the powerspectrum is superior regardless of γ , and the minimum value of γ which leads to detection (ie $\text{SNR}_2^{\Phi} > 1$) is lower for the powerspectrum than the bispectrum.

6. Conclusions

This paper has considered the potential advantages in using the bispectrum to analyse data from weakly non-linear systems driven with deterministic sinusoidal signals.

The bispectrum detects signals that are quadratically phase coupled (QPC) and suppresses those that are not, which is why it is of interest for identifying system non-linearity. However, it has been shown that care must be taken in the averaging process with systems excited deterministically in order to exploit this property of the bispectrum. It has been shown that if the signal at $F_1 + F_2$ is not quadratically phase coupled to those at F_1 and F_2 , it will be suppressed by the bispectrum if one or more of the phases of the signals can be randomized with respect to the others in different response records. Dividing a single long record into many shorter segments and averaging the bispectra obtained from each segment does not achieve this; neither does any method where the excitation is continuous between records. The bispectrum does suppress the non-quadratically-phase coupled signal at $F_1 + F_2$ if the phases of the exciting signals are synchronized with the start of each record and the start times are randomized; however in this case, the records could be averaged directly to achieve the same result. The bispectrum does have a unique advantage for detecting quadratic phase coupling with periodic excitation is the phases of one or both of the exciting signals are (independently) randomized with respect to the start of each record.

The merit of using the bispectrum to mitigate noise in the signal was also considered, for a sinusoidally excited system in the presence of Gaussian noise. The expectation values of the estimated bispectrum were evaluated along with their variance and compared to the same values for the powerspectrum. It was found that although the expected value of the noise for the bispectrum estimator was in principle zero, if the effect of the variance of the noise was taken into account then the powerspectrum outperforms the bispectrum for this particular application.

A. Expectation values

This appendix covers the derivation of expectation values useful to the calculations of the main body of the work.

A.1. Product of two noise signals in the frequency domain

There are two values of interest, the expectation value of the product of the noise in the frequency domain with its conjugate, and the square of the frequency domain signal

(without the conjugate). The former is derived in section 4.3 and the latter here:

$$\begin{aligned}
\mathbb{E}[Q(f_n)Q(f_n)] &= \mathbb{E}\left[\frac{1}{N}\sum_{l=1}^N\left\{q(t_l)e^{-i2\pi nl/N}\right\}\frac{1}{N}\sum_{m=1}^N\left\{q(t_m)e^{-i2\pi nm/N}\right\}\right] \\
&= \frac{1}{N^2}\sum_{l,m=1}^N\left\{e^{(-i2\pi n(m+l)/N)}\mathbb{E}[q(t_l)q(t_m)]\right\} \\
&= \frac{1}{N^2}\sum_{m=1}^N\left\{e^{(-i4\pi nm/N)}\mathbb{E}[q^2(t_m)]\right\} \\
&= \frac{\sigma^2}{N^2}\sum_{m=1}^N\left\{e^{(-i4\pi nm/N)}\right\} \\
&= 0. \tag{A.1}
\end{aligned}$$

The final step follows from the summation over m being over a regular distribution on the real-imaginary plane and consequently summing to zero.

A.2. Product of four noise signals in the frequency domain

Consider the expectation value of the product of four noise signals in the frequency domain, where two are complex conjugates, $\mathbb{E}[Q_i(f)Q_j^*(f)Q_k^*(f)Q_l(f)]$. As the variables are independent with regard data set, any combination of indices i, j, k, l where one differs from the others gives value multiplied by $\mathbb{E}[Q(f)] = 0$. And so only cases where all four indices are equal ($i = j = k = l$), or there are two pairs of equal indices are of interest ($i = j \neq k = l, i = k \neq j = l, i = l \neq j = k$). The first case ($i = j = k = l$) gives

$$\begin{aligned}
\mathbb{E}[Q(f_n)Q^*(f_n)Q^*(f_n)Q(f_n)] &= \mathbb{E}[\mathcal{F}(q(t))\mathcal{F}(q(t))^*\mathcal{F}(q(t))^*\mathcal{F}(q(t))] \\
&= \frac{1}{N^4}\sum_{m,p,r,s=0}^{N-1}\left\{\mathbb{E}[q(t_m)q(t_p)q(t_r)q(t_s)]e^{-i(2\pi n(m+s-p-r))/N}\right\} \\
&= \frac{1}{N^4}\left(N\mathbb{E}[q^4(t)] + N(N-1)\mathbb{E}[q^2(t)]\mathbb{E}[q^2(t)]\right. \\
&\quad \left.+ \sum_{m=0}^{N-1}\sum_{p=0, p \neq m}^{N-1}\left\{\mathbb{E}[q^2(t)]\mathbb{E}[q^2(t)]e^{-i(2\pi n(2m-2p))/N}\right\}\right) \tag{A.2}
\end{aligned}$$

The summation can be rewritten in terms of summations over complete sets of indices:

$$\begin{aligned}
\sum_{m=0}^{N-1}\sum_{p=0, p \neq m}^{N-1}\left\{e^{(-i2\pi n(2m-2p))/N}\right\} &= \sum_{m=0}^{N-1}\sum_{p=0}^{N-1}\left\{e^{(-i2\pi n(2m-2p))/N}\right\} - \sum_{m=0}^{N-1}\sum_{p=0}^{N-1}1 \\
&= -N \tag{A.3}
\end{aligned}$$

. $E[q^2(t)]$ and $E[q^4(t)]$ are given in section 4.3 and so

$$\begin{aligned}
E [Q(f_n)Q^*(f_n)Q^*(f_n)Q(f_n)] &= \frac{1}{N^4} \left\{ NE[q^4(t)] + 2N(N-1)E[q^2(t)]E[q^2(t)] \right. \\
&\quad \left. - NE[q^2(t)]E[q^2(t)] \right\} \\
&= \frac{1}{N^4} \left(3N\sigma^4 + 2N^2\sigma^4 - 3N\sigma^4 \right) \\
&= \frac{2}{N^2}\sigma^4
\end{aligned} \tag{A.4}$$

There are two possibilities for cases where there are two pairs of identical indices, either there are two expectation values of the noise multiplied by its conjugate ($i = j \neq k = l$ or $i = k \neq j = l$) in which case from Eq. (35):

$$E [Q_i(f_n)Q_i^*(f_n)Q_j^*(f_n)Q_j(f_n)] = \frac{1}{N^2}\sigma \tag{A.5}$$

or there is one expectation value of the noise squared and one of the conjugate multiplied by itself ($i = l \neq j = k$), from Eq. (36):

$$E [Q_i(f_n)Q_i(f_n)Q_j^*(f_n)Q_j^*(f_n)] = 0 \tag{A.6}$$

B. Notable summations

In order to evaluate the expected value of the powerspectrum of the average signal the following summations are required:

$$\sum_{i,j,k,l=1}^M \left\{ X^{(S)}(F_3)X^{(S)*}(F_3)X^{(S)*}(F_3)X^{(S)}(F_3) \right\} = \frac{S_3^4}{16} \tag{B.1}$$

$$\begin{aligned}
\sum_{i,j,k,l=1}^M \left\{ X^{(S)}(F_3)X^{(S)*}(F_3) \left\{ E[Q_k^*(F_3)Q_l(F_3)] + E[Q_l^*(F_3)Q_j(F_3)] \right. \right. \\
\left. \left. + E[Q_i^*(F_3)Q_k(F_3)] + E[Q_i^*(F_3)Q_j(F_3)] \right\} \right\} &= S_3^2 M^3 E[Q(F_3)^*Q(F_3)] \\
&= \frac{M^3}{N} S_3^2 \sigma^2
\end{aligned} \tag{B.2}$$

and

$$\begin{aligned}
\sum_{i,j,k,l=1}^M \left\{ E[Q_i(F_3)Q_j^*(F_3)Q_k^*(F_3)Q_l(F_3)] \right\} &= ME [Q(F_3)Q^*(F_3)Q^*(F_3)Q(F_3)] \\
&\quad + 2M(M-1)E [Q(F_3)Q^*(F_3)] E [Q(F_3)Q^*(F_3)] \\
&= M \frac{2}{N^2}\sigma^4 + 2M(M-1) \left(\frac{1}{N}\sigma^2 \right)^2
\end{aligned} \tag{B.3}$$

References

- [1] O. Buck, W.L. Morris, and J. M. Richardson. Acoustic harmonic generation at unbounded interfaces and fatigue cracks. *Applied Physics Letters*, 33:371–373, 1978.
- [2] W. L. Morris, O. Buck, and R. V. Inman. Acoustic harmonic generation due to fatigue damage in high-strength aluminium. *Journal of Applied Physics*, 50:6737–6741, 1979.
- [3] P. B. Nagy. Fatigue damage assessment by nonlinear ultrasonic materials characterisation. *Ultrasonics*, 36:375–381, 1998.
- [4] D. Donskoy, A. Sutin, and A. Ekimov. Nonlinear acoustic interaction on contact interfaces and its use for nondestructive testing. *NDT&E International*, 34:231–238, 2001.
- [5] J.N. Sundermeyer and R.L. Weaver. On crack identification and characterization in a beam by non-linear vibration analysis. *Journal of Sound and Vibration*, 183:857–871, 1995.
- [6] N. Pugno, C. Surace, and R. Ruotola. Evaluation of the non-linear dynamic response to harmonic excitation of a beam with several breathing cracks. *Journal of Sound and Vibration*, 235:749–762, 2000.
- [7] S. L. Tsyfansky and V. I. Beresnevich. Non-linear vibration method for detection of fatigue cracks in aircraft wings. *Journal of Sound and Vibration*, 236:49–60, 2000.
- [8] S. A. Neild, M. S. Williams, and P. D. McFadden. Nonlinear vibration characteristics of damaged concrete beams. *Journal of Structural Engineering-ASCE*, 129:260–268, 2003.
- [9] K. E.-A. Van Den, P. A. Johnson, and A. Sutin. Nonlinear elastic wave spectroscopy (news) techniques to discern material damage, part i: Nonlinear wave modulation spectroscopy (nwms). *Research in Nondestructive Evaluation*, 12:17–30, 2000.
- [10] P. Duffour, M. Morbidini, and P. Cawley. A study of the vibro-acoustic modulation technique for the detection of cracks in metals. *Journal of the Acoustical Society of America*, 119:1463–1475, 2006.
- [11] C. R. P. Courtney, B. W. Drinkwater, S. A. Neild, and P. D. Wilcox. Factors affecting the ultrasonic intermodulation crack detection technique using bispectral analysis. *NDT&E International*, 41:223–234, 2008.
- [12] D. W. Yan, B. W. Drinkwater, and S. A. Neild. Measurement of the ultrasonic nonlinearity of kissing bonds in adhesive joints. *NDT&E International*, 42:459–466, 2009.
- [13] K. Worden, C.R. Farrar, J. Haywood, and M. Todd. A review of nonlinear dynamics applications to structural health monitoring. *Structural Control and Health Monitoring*, 15:540–567, 2008.
- [14] Y. C. Kim and E. J. Powers. Digital bispectral analysis and its applications to nonlinear wave interactions. *IEEE Transactions on Plasma Science*, 7:120–131, 1979.
- [15] K. Hasselmann, W. Munk, and G. Macdonald. Bispectra of ocean waves. In M. Rosenblatt, editor, *Proceedings of the Symposium on Time Series Analysis*, 1963.
- [16] M. D. Godfrey. An exploratory study of the bi-spectrum of economic time series. *Applied Statistics*, 14:48–69, 1965.
- [17] P. J. Huber, B. Kleiner, and T. Gasser. Statistical methods for investigating phase relations in stationary stochastic processes. *IEEE Transaction on Audio and Electroacoustics*, AU19:78–86, 1971.
- [18] T. P. Barnett, L. C. Johnson, P. Naitoh, N. Hicks, and C. Nute. Bispectrum analysis of electroencephalogram signals during waking and sleeping. *Science*, 172:401–402, 1971.
- [19] K. S. Lii, M. Rosenblatt, and C. Van Atta. Bispectral measurements in turbulence. *Journal of Fluid Mechanics*, 77:45–62, 1976.
- [20] M. Rosenblatt. Estimation of the bispectrum. *The Annals of Mathematical Statistics*, 36:1120–1136, 1965.
- [21] M. R. Raghuveer and C. L. Nikias. Bispectrum estimation: A parametric approach. *IEEE Transaction on Acoustics, Speech, and Signal Processing*, ASSP13:1213–1230, 1985.
- [22] C. L. Nikias and M. R. Raghuveer. Bispectrum estimation: A digital signal processing framework. *Proceedings of the IEEE*, 75:869–891, 1987.
- [23] J.M. Nichols, P. Marzocca, and A. Milanese. On the use of the auto-bispectral density for detecting quadratic nonlinearity in structural systems. *Journal of Sound and Vibration*, 312:726–735, 2008.
- [24] J. W. A. Fackrell, P. R. White, J. K. Hammond, and R. J. Pinnington. The interpretation of the bispectra of vibration signals-i. theory. *Mechanical Systems and Signal Processing*, 9:257–266, 1995.
- [25] J. W. A. Fackrell, P. R. White, J. K. Hammond, and R. J. Pinnington. The interpretation of the bispectra of vibration signals-ii. experimental results and applications. *Mechanical Systems and Signal Processing*, 9:257–266, 1995.

- [26] I. M. Howard. Higher-order spectral techniques for machine vibration condition monitoring. *Proceedings of the Institution of Mechanical Engineers, G*, 211:211–219, 1997.
- [27] W. B. Collis, P. R. White, and J. K. Hammond. Higher-order spectra: The bispectrum and trispectrum. *Mechanical Systems and Signal Processing*, 12:375–394, 1998.
- [28] M. Boltežar and N. Jakšić. Dynamical behaviour of the planar non-linear mechanical system-part ii: Experiment. *Journal of Sound and Vibration*, 226:941–953, 1999.
- [29] Jyoti K. Sinha. Higher order spectra for crack and misalignment identification in the shaft of a rotating machine. *Structural Health Monitoring*, 6:325–334, 2007.
- [30] A. Rivola and P. R. White. Bispectral analysis of the bilinear oscillator with application to the detection of fatigue cracks. *Journal of Sound and Vibration*, 216:889–910, 1998.
- [31] A. J. Hillis, S. A. Neild, B. W. Drinkwater, and P. D. Wilcox. Global crack detection using bispectral analysis. *Proceedings of Royal Society*, 462:1515–1530, 2006.
- [32] Jerry M. Mendel. Tutorial on higher-order statistics (spectra) in signal processing and system theory: theoretical results and some applications. *Proceedings of the IEEE*, 79:278–305, 1991.
- [33] K. S. Lii and K. N. Helland. Cross-bispectrum and variance estimation. *ACM Transactions on Mathematical Software*, 7:284–294, 1981.
- [34] S. Elgar and R. T. Guza. Statistics of bicoherence. *IEEE Transaction on Acoustics, Speech, and Signal Processing*, 36:1667–1668, 1988.
- [35] B. O. Peirce and R. M. Foster. *A Short Table of Integrals*. Ginn and Company, 4th edition, 1956.